





## Sedimentary DNA and molecular evidence for early human occupation of the Faroe Islands

Lorelei Curtin<sup>1</sup><sup>✉</sup>, William J. D'Andrea<sup>1</sup><sup>✉</sup>, Nicholas L. Balascio<sup>2</sup>, Sabrina Shirazi<sup>3</sup>, Beth Shapiro<sup>3</sup>, Gregory A. de Wet<sup>4,6</sup>, Raymond S. Bradley<sup>4</sup><sup>4</sup> & Jostein Bakke<sup>5</sup><sup>5</sup>

The Faroe Islands, a North Atlantic archipelago between Norway and Iceland, were settled by Viking explorers in the mid-9th century CE. However, several indirect lines of evidence suggest earlier occupation of the Faroes by people from the British Isles. Here, we present sedimentary ancient DNA and molecular fecal biomarker evidence from a lake sediment core proximal to a prominent archaeological site in the Faroe Islands to establish the earliest date for the arrival of people in the watershed. Our results reveal an increase in fecal biomarker concentrations and the first appearance of sheep DNA at 500 CE (95% confidence interval 370–610 CE), pre-dating Norse settlements by 300 years. Sedimentary plant DNA indicates an increase in grasses and the disappearance of woody plants, likely due to livestock grazing. This provides unequivocal evidence for human arrival and livestock disturbance in the Faroe Islands centuries before Viking settlement in the 9th century.

<sup>1</sup>Lamont-Doherty Earth Observatory, Palisades, NY, USA. <sup>2</sup>Department of Geology, William & Mary, Williamsburg, VA, USA. <sup>3</sup>Department of Ecology and Evolutionary Biology, University of California, Santa Cruz, CA, USA. <sup>4</sup>Department of Geosciences, University of Massachusetts, Amherst, MA, USA. <sup>5</sup>Department of Earth Science and Bjerknes Centre for Climate Research, University of Bergen, Bergen, Norway. <sup>6</sup>Present address: Department of Geosciences, Smith College, Northampton, MA, USA. ✉email: [lcurtin@uwyo.edu](mailto:lcurtin@uwyo.edu); [dandrea@ldeo.columbia.edu](mailto:dandrea@ldeo.columbia.edu)

The Faroe Islands, located between Iceland, Norway, and the British Isles, were a stepping stone for Viking exploration across the North Atlantic. The general consensus is that the Norse were the first humans to settle the Faroe Islands, and accordingly, the earliest archaeological structures on the Faroes date between 800–900 CE<sup>1,2</sup>. This is consistent with the timing of a broader Norse expansion during the Viking Age (~800–1100 CE), when the Norse established new settlements on the Faroes, Iceland, Greenland, and beyond to North America.

Despite nearly all archaeological evidence pointing toward the initial Norse occupation of the Faroes in the 9th century, there is indirect evidence that suggests that people may have settled the Faroe Islands before the main phase of Norse settlement. In 825 CE, an Irish monk named Dicuil mentioned in writing that some northern islands had been settled by hermits for at least one hundred years<sup>3</sup>. Additionally, many place names in the Faroes derive from Celtic words<sup>4</sup> and Celtic grave markings have been identified on the islands<sup>2,5</sup>. The genetics of the modern population of Faroese people is strongly asymmetric between the paternal and maternal ancestry; while the paternal lineage is primarily Scandinavian, the maternal lineage is primarily from the British Isles<sup>6</sup>. While other regions of the North Atlantic also show this asymmetry, the Faroe Islands have the highest proportion of British Isles maternal ancestry and the highest level of genetic asymmetry<sup>6</sup>, suggesting that there was potentially a pre-existing population of predominately British Isles descent. However, whether or not Dicuil's text refers to the Faroes is controversial<sup>7</sup> and place-name, grave-marking, and modern population genetic evidence is not inconsistent with the hypothesis that the Norse were the initial settlers. Indeed, by 800 CE, the Vikings were already active in the British Isles. They were already influenced by Celtic culture, and could have brought wives from the British Isles to the Faroe Islands. Almost all of the evidence for early human arrival to the Faroe Islands is inconclusive, and direct physical evidence is lacking.

Debate regarding the early settlement of the Faroes was reignited upon the discovery of a few charred barley grains with a weighted mean age of 351–543 CE at the Å Sondum archaeological site on the island of Sandoy<sup>8</sup>. The processing of barley, along with the anthropogenic ash deposit in which the grains were found, suggest that some form of human settlement existed on the Faroes prior to the arrival from the Norse. However, there has been no additional archaeological evidence to corroborate the early arrival of humans to the Faroes.

Environmental records from sediment cores can provide valuable constraints concerning the first arrival of humans to the Faroe Islands. While the nature of archaeological records causes them to be temporally fragmentary, sedimentary archives provide continuous records of the environmental history of a landscape. The environmental record of human land-use disturbance in the Faroes has been investigated primarily through the analysis of pollen and plant macrofossils from the lake and bog sediments<sup>9–16</sup>. Pollen and macrofossil analyses have shown that earlier in the Holocene period, the vegetation of the Faroes included stands of woody vegetation, including *Betula* (birch), *Juniperus* (juniper), and *Salix* (willow)<sup>10,17</sup>. The reduction in woody vegetation cover could be due to regional cooling and drying<sup>18</sup>, however, it is thought that major vegetation change on the Faroes only occurred after the arrival of humans, when grazing animals eliminated the woody vegetation. The early (4250 BP) appearance of *Plantago lanceolata* in the Faroes was originally believed to have been due to very early human settlement<sup>19</sup>. However, *Plantago lanceolata* pollen occurs in Iceland prior to the well-established Norse settlement period, which suggests that it cannot be used to confirm the early human settlement of North Atlantic islands. Cereal grain pollen, which could only occur on the Faroes after the initiation of agriculture, was identified in previous sediment cores and dated to ~1500 BP<sup>11</sup>, leading the authors to propose a pre-Norse occupation of the islands.

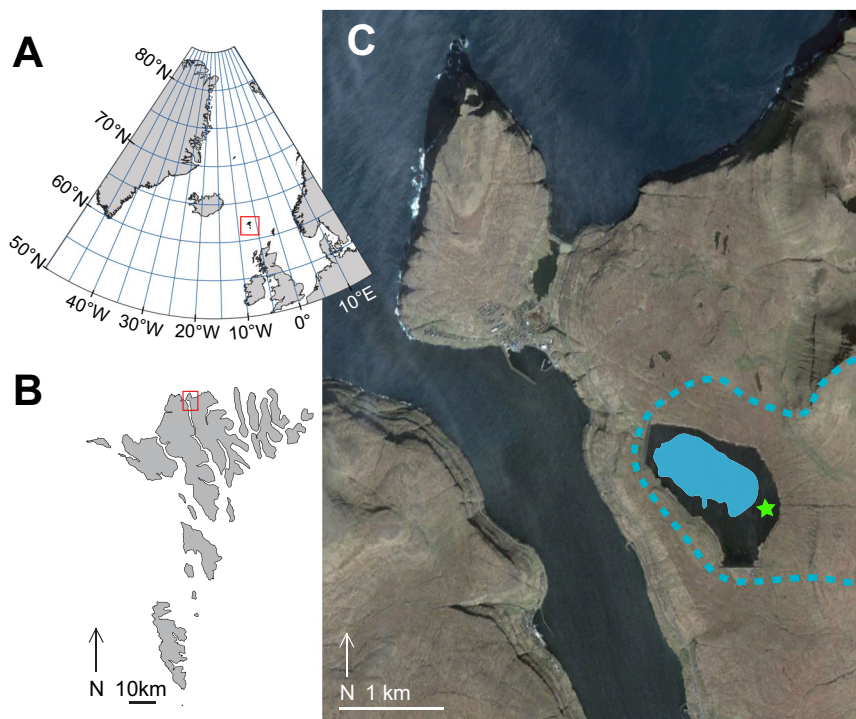


**Fig. 1 Maps of the North Atlantic, Faroe Islands, and study location.** **a** Map of North Atlantic region, with the Faroe Islands in red box. **b** Map of the Faroe Islands, with the Eiði region in red box. **c** Eiðisvatn, with blue fill showing the approximate extent of the lake before the emplacement of the hydroelectric dam, green star showing the approximate location of Argisbrekka. Blue dashed line indicates Eiðisvatn watershed boundary. Satellite imagery from Google Earth, Image ©2021 Maxar Technologies, Landsat/Copernicus.

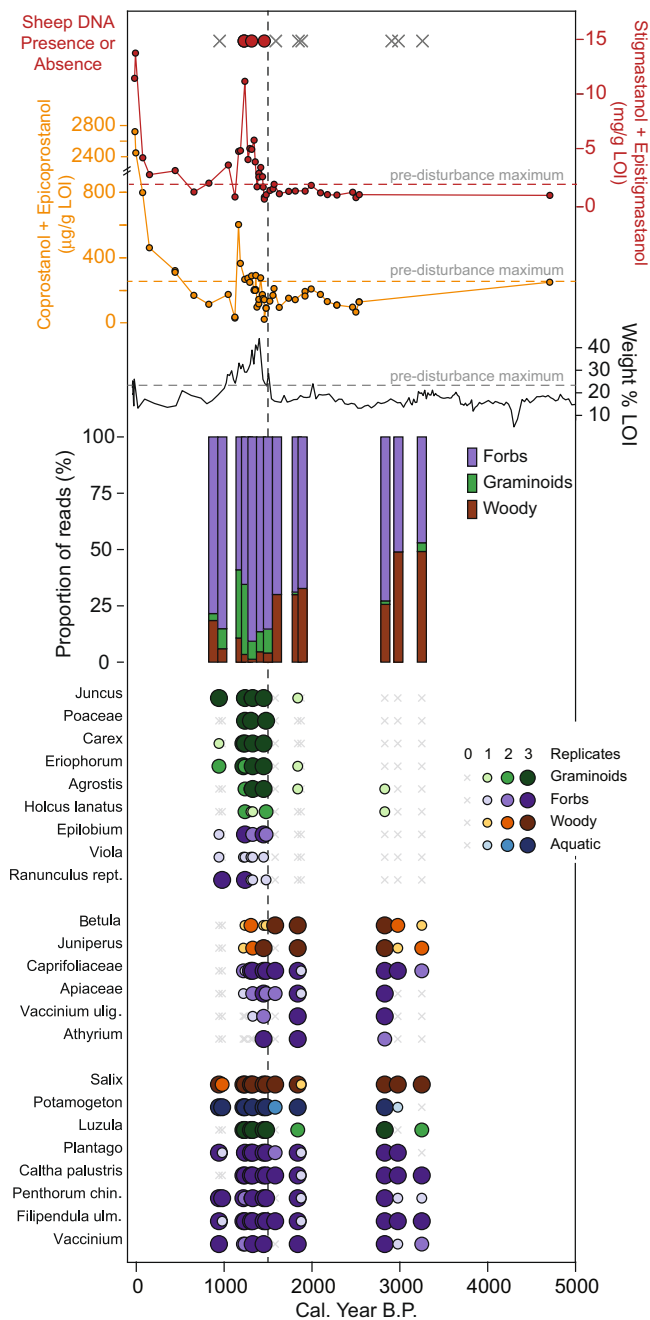


**Fig. 2** Sheep DNA presence, fecal sterol biomarker concentrations, and plant genus DNA presence in Eiðisvatn lake sediment. A representative subset of plant genera are included; the complete dataset can be found in Supplementary Figure 3. Plant DNA data points are scaled by size and color relative to the number of PCR replicates in which the specific plant genus was positively identified (threshold of 5 reads or greater). Grey dashed vertical line indicates sedimentary horizon for human arrival, when sheep DNA first appears, fecal biomarker concentrations increase, and plant DNA reveals a turnover in the plant community. The top section of plant data show genera that increased in frequency after the introduction of livestock. The middle section of plant data show genera that decreased in frequency after the introduction of livestock. The bottom section of plant data show plant genera that remain unchanged throughout the introduction of livestock.

However, the age models from these studies are far too uncertain to constrain human arrival, because livestock grazing also resulted in widespread erosion. This erosion supplied old organic material into the lakes and bogs, which makes it difficult to firmly establish radiocarbon-based age control on sedimentary environmental records without large numbers of dates. As a result, our understanding of the first arrival of plants that were introduced by humans is limited.

Here, we present a lake sediment record of fecal biomarkers and sedimentary ancient DNA that can unequivocally identify the signature of human presence on the Faroe Islands. We use these unambiguous markers for the presence of livestock on the Faroe Islands, together with a combination of extensive radiocarbon dating and tephrochronology, to determine that the arrival of humans and livestock to the Faroe Islands occurred approximately 300 years before the Norse arrival to the Faroes. Our study site, Eiðisvatn on the island of Eysturoy, is proximal to a Norse shieling, a summer farm settlement, called Argisbrekka<sup>20</sup> (Fig. 1). Argisbrekka was the shieling associated with the village of Eiði, which was an important coastal Viking settlement site. Argisbrekka was excavated in 1985–1987 just prior to the damming of Eiðisvatn, which expanded the lake area and flooded the site. The proximity of our study site to a major archaeological site, and the village of Eiði, places our record in the context of the local archaeological record.

Fecal biomarkers, including coprostanol and  $\beta$ -stigmasterol, are lipid molecules produced in the digestive tract of mammals<sup>21</sup>, and can be used to identify the presence of human and livestock populations in a watershed<sup>22,23</sup>. These degradation products of cholesterol and sitosterol are found in higher than background concentrations in the feces of mammals. Many environmental tracers that are used to indicate the human presence and land use, such as pollen, charcoal, and sediment accumulation rates, can be influenced by natural landscape ontogeny and climate variability; however, fecal biomarkers provide unmistakable evidence for the presence of humans and livestock. This tool proves particularly useful in the Faroe Islands, where all mammals were originally introduced by humans.

The emergence of next-generation DNA sequencing technology has allowed the application of metabarcoding to sedimentary archives. Sedimentary ancient DNA (*sedaDNA*) metabarcoding allows detection of changes in local plant and mammal community composition through time<sup>24</sup>. Plant *sedaDNA* can be used to reconstruct plant communities in the past<sup>25–27</sup>, while the identification of mammal DNA, particularly livestock DNA, in sediment provides irrefutable evidence for the presence of human-introduced species in a watershed<sup>28</sup>. With the combination of plant and mammal *sedaDNA* and fecal biomarkers, we conclude that humans introduced livestock to the Faroe Islands at least 300 years prior to Norse settlement.

## Results

**Age model and sediment properties.** We used 10 radiocarbon ages (Supplementary Table 1) and 5 geochemically fingerprinted tephra layers (Supplementary Table 1, Supplementary Fig. 1) as constraints for an age model for Eiðisvatn sediments<sup>18</sup> (Supplementary Fig. 2). We used Bacon, a Bayesian age modeling software package in R, to make the age model and calculate the age uncertainties for each interval in the sediment core. The age model shows nearly continuous sedimentation rates throughout the Holocene, with a slight increase in sedimentation rate during an interval with high loss-on-ignition values (LOI) and anomalously old radiocarbon ages. The onset of the disturbance interval, which was first proposed to occur ~2.4 ka<sup>18</sup> has been

revised to ~1.5 ka based on the addition of one radiocarbon date, removal of bulk sediment dates, and the tentative identification of the Landnám tephra, which has a known age of 877 CE  $\pm$  1 yr<sup>29</sup>.

LOI, which represents the organic matter content of sediment, ranges from ~10 to 40% throughout the sediment core. LOI slowly increases from the bottom of the core until a sharp increase occurs ~53 cm depth (Fig. 2), which corresponds to 1514 BP (95% confidence range from 1415 to 1670 BP) according to our age model. LOI remains above 20% until 29 cm. During this high-LOI interval, eight radiocarbon samples yield age reversals (Supplementary Fig. 2). We interpret this period of increased organic sedimentation and anomalously old radiocarbon dates as evidence for enhanced erosion of peaty soils in the catchment, contributing organic-rich sediment containing older plant macrofossils to the lake<sup>18</sup>. This interpretation is supported by an increase in the concentration of terrestrially derived leaf wax biomarkers in the lake sediment<sup>18,30</sup> an increase in the carbon isotope values of those biomarkers<sup>18</sup>, and an increase in the concentration of soil-derived glycerol dialkyl glycerol tetraethers<sup>30</sup>.

**Fecal biomarkers.** We identified and quantified fecal stanols in all samples. We summed 5 $\beta$ -stigmastan-5 $\beta$ -ol (stigmastanol) and its epimer 5 $\beta$ -stigmastan-5 $\alpha$ -ol (epistigmastanol), and 5 $\beta$ -cholestan-5 $\beta$ -ol (coprostanol) and its epimer 5 $\beta$ -cholestan-5 $\alpha$ -ol (epicoprostanol), which indicate the presence of mammals in the watershed<sup>31</sup>. We report fecal sterol concentrations normalized to the amount of organic matter (wt % LOI) such that the record is not influenced by the increase in organic sedimentation during the landscape disturbance interval. The concentration of both stigmastanol and coprostanol (and their epimers) increase during the disturbance interval at 50 cm depth, or 1433 BP (95% confidence range from 1317 to 1565 BP), exceeding their pre-disturbance maxima (Fig. 2). Both decline following the main disturbance interval, and then increase to their highest values in modern samples.

**Sedimentary ancient DNA.** We extracted DNA from 14 sediment samples taken from eleven depths spanning the disturbance interval. Samples were shipped in two batches to the Paleogenomics Laboratory at the University of California Santa Cruz, where they were processed for *sedDNA* in two batches. Processing took place in the specialized ancient DNA facility and followed protocols developed specifically for working with degraded DNA. From each extract, we amplified plant and mammalian DNA using metabarcoding, using three replicate PCRs (see Methods) per metabarcode. For each replicate PCR, we set a minimum read threshold of five (at least five reads per taxon were necessary to consider that taxon “present”) so as to minimize false positives due, for example, to sequencing error and background contamination.

Following the initial metabarcoding experiment for mammal DNA, the first batch of six samples (AA-FF; see Supplementary Data 1) amplified only low levels of human DNA. We hypothesized that storage conditions of this first batch of samples may have increased DNA degradation in these samples, to which the mammalian metabarcode is more sensitive than the plant metabarcode due to a longer length of amplified product. Of the eight samples in the second batch (II-PP; see Supplementary Data 1), three samples contained Sheep DNA in all three replicate PCRs, with between 7521 and 355,512 reads assigned to sheep. All three positive sheep samples were taken from the main disturbance interval, with the oldest sheep DNA identified at 50.88 cm, or 1458 BP (95% confidence range from 1580 to 1343 BP) (Fig. 2). One of the sheep-positive samples also contained

*Cervid* (deer) DNA in all three PCR replicates, with between 40 and 318 reads, human DNA in 1 PCR replicate (1228 reads), and *Bos taurus* (cattle) DNA in 1 replicate (63 reads). The low read counts suggest that these identifications may have resulted from either contamination (human and *Cervid*) or misalignment between bovinds (*Bos taurus*). One additional sheep-positive sample contained human DNA in one PCR replicate (1031 reads).

We identified 40 plant taxa across the 14 *sedDNA* samples (Fig. 2, S3). Unlike the mammalian DNA, there was no difference in preservation between batches. This could be due to a higher abundance of plant DNA in the extracts or the smaller average amplicon size for plants compared to mammals or a combination of the two. We identified the resulting plant barcodes to the genus level.

We observed that four types of graminoids, including *Juncus* (rushes), *Eriophorum* (cottongrass/sedge), *Carex* (sedges), and *Agrostis* (bentgrass), are more frequently identified after the onset of increased organic sedimentation, coeval with the first positive identification of sheep DNA (Fig. 2). Two types of forbs, including *Ranunculus* (buttercups, spearworts) and *Epilobium* (willowherbs, spike primrose), also become more frequent at the same time. Across the same transition, several genera become less frequently identified, including woody plants *Betula* (birch) and *Juniperus* (juniper), and forbs *Caprifoliaceae* (honeysuckle), and *Apiaceae* (umbellifers).

## Discussion

We identify the sedimentary horizon with the first appearance of sheep DNA and an increase in the concentration of fecal biomarkers within 1 cm of sediment deposition in the core (equivalent to ~25 years) (Fig. 2). The co-occurrence of these two independent molecular indicators for the presence of livestock in the watershed provides conclusive evidence for human arrival in the Eiðisvatn catchment by this time. The age of this horizon is 1433–1458 BP (492–517 CE) based on the first detection of sheep DNA and the initial increase of stigmastanol, with a minimum age of 1317 BP (633 CE) based on a 95% confidence interval (Fig. 3).

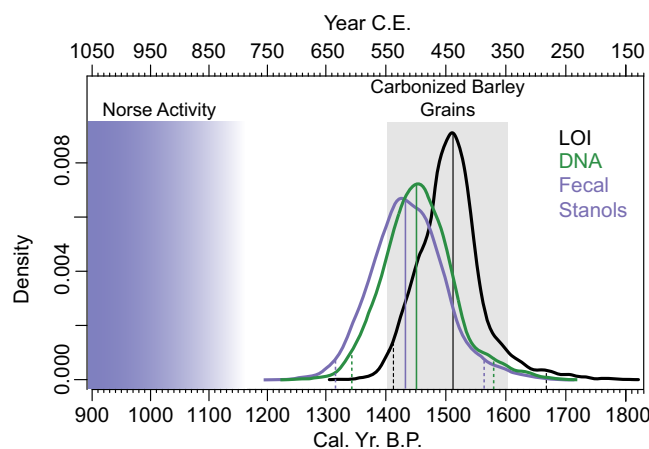


**Fig. 3 Timing of human settlement on the Faroe Islands.** Probability density functions for the ages of first evidence for the introduction of livestock based on Bacon age model for each of the three livestock indicators. Vertical solid lines indicated weighted mean age from all age model runs, and dashed vertical lines indicate 95% confidence intervals. Grey vertical bar shows the calibrated ages for the carbonized barley grains from Sandoy<sup>8</sup>, and blue vertical bar shows the period of Norse activity on the Faroes.



The archaeological excavation at Argisbrekka provides important context for interpreting these data. Argisbrekka was a shieling, or a temporary summer settlement for grazing sheep. Radiocarbon dating of the archaeological structures suggested that the Viking-age shieling was originally built in the mid-9th century, and after multiple phases of activity, was abandoned in the mid-11th century<sup>20</sup>. The initial appearance of sheep DNA and increased fecal biomarkers pre-dates the first documented usage of the Argisbrekka site by the Norse by approximately 300 years (Fig. 3). The magnitude of stigmastanol increase is greater than that of coprostanol. Sheep feces contain larger amounts of stigmastanol than coprostanol (approximately 6:1<sup>31</sup>) compared to omnivores such as pigs (approximately 2:1<sup>31</sup>) or humans, consistent with the notion that sheep likely outnumbered humans and were more important contributors of feces to the landscape.

The modern plant community on the Faroes is dominated by herbaceous plants, including grasses, sedges, and rushes. However, Holocene pollen records show that woody and shrub vegetation was in higher abundance earlier in the Holocene<sup>11</sup>. Shrubs and other woody vegetation currently grow only in areas that are not easily reached by sheep, which graze extensively across the Faroes. Pre-settlement vegetation was thought to include small stands of *Salix*, *Empetrum*, *Calluna vulgaris*, and *Betula nana*<sup>12,19</sup>. Stumps of *Betula pubescens* and *Juniperus* macrofossils were discovered at the Argisbrekka site and dated to 4450 BP<sup>32</sup>, however, pollen analysis from the site lacks pollen from these species, suggesting that the presence or absence of woody taxa may not be accurately represented by pollen analysis<sup>11,12,33</sup>. It is thought that these stands of woody vegetation likely persisted until human settlement<sup>13</sup>.

Our *sedDNA* results suggest the disappearance of woody vegetation, including *Betula* and *Juniperus*, shortly after the first appearance of sheep on the landscape (Fig. 2). This is in agreement with nearby pollen and macrofossil records, which show a reduction in these taxa coeval with the onset of human settlement, as identified by increased grass pollen and microcharcoal fragments<sup>10,12</sup>. However, *Salix* DNA persists throughout the human disturbance interval.

Our evidence for first human arrival aligns with the charred barley grain recovered from the Å Sondum site on Sandoy (8), confirming that humans had arrived in the Faroe Islands and had at least temporary settlements prior to Norse arrival (Fig. 3). While this is earlier than the Viking-age archaeology, it aligns well with some other published paleobotanical records for human settlement<sup>13</sup>. Closest to Eiðisvatn lake, at Heimavatn (Eiði bog), Hannon et al., 2005<sup>14</sup> found *Hordeum* (barley) pollen along with large wild Gramineae pollen and macrocharcoal fragments at 570 CE. Elsewhere in the Faroes, cereal grain pollen has been documented in the 600s CE<sup>34</sup>. However, the previously published paleoecological records are derived from very poorly dated sequences, which inhibits comparison between the pollen reconstructions, our new data, and the archaeological data.

The Landnám tephra was deposited widely across the North Atlantic in 877 CE<sup>29</sup>, making it a useful stratigraphic marker for the Viking settlement period<sup>35</sup>. We tentatively identify the Landnám tephra in Eiðisvatn sediments (Supplementary Fig. 1, Supplementary Table 2) at a depth of 33 cm, which is stratigraphically 17 cm above our first evidence for human presence on the Faroe Islands. While the geochemistry of our Landnám tephra samples match the range of values previously reported for Landnám tephra samples from other locations in the Faroes, the TiO<sub>2</sub> values of our samples are offset from the mean of TiO<sub>2</sub> from previously published samples (Supplementary Figure 1). If we exclude the Landnám tephra from our age model, the occurrence of this ash deposit dates to 875 CE (95% confidence interval of 871–879 CE), and the age of our evidence for human presence

does not change significantly (Supplementary Fig. 4, Supplementary Table 3).

## Conclusions

Using a combination of fecal biomarkers and sedimentary ancient DNA, we show conclusive evidence that humans had introduced livestock to the Faroe Islands three to four centuries before the Viking-age Norse settlement period that is widely documented in the archaeological record. We constrain the most likely timing of human arrival to the Eiðisvatn catchment to ~500 CE, approximately 350 years before Viking Age settlements on the Faroes. The latest possible arrival allowed by the 95% CI of our bayesian age model is ~630 CE, approximately 200 years before the earliest documented Norse activity began on the Faroes. While historical documents suggest that there were Celtic monks on the Faroe Islands prior to the Viking Age<sup>3</sup>, there is a lack of any archaeological evidence for human activity from this time period on the Faroe Islands beyond a few charred barley grains, and our evidence cannot directly speak to who these early settlers were. However, it is thought that the Norse were late adopters of sailing technology, making it difficult for them to have reached the Faroes prior to the generally accepted date for their adoption of the sail sometime between 750 and 820 CE<sup>36–38</sup>. This suggests that the early Faroese settlers were not Norse, however, the identity of these early North Atlantic explorers remains an open question. We also show that widespread erosion of fragile shrubland has influenced our understanding of the timing of late Holocene vegetation development on the Faroes, and that the transition from shrubland to grass/sedge-dominated peatlands was likely driven by anthropogenic and livestock activity and not by late Holocene climate changes.

## Materials and methods

**Lake sediment cores and chronology.** We recovered sediment cores from the deepest part of Eiðisvatn in August of 2015. Sampling permission was not required. We recovered two gravity cores to preserve the sediment/water interface. We sampled the upper 10 cm of one gravity core, EI-D-01-15 (83.7 cm), in the field, and left EI-D-02-15 (100.7 cm) whole. We collected and transported a percussion-piston core (EI-P-01-15, 281.5 cm) whole. We split, imaged, and scanned one surface core (EI-D-01-15) and the piston core (EI-P-01-15) using an ITRAX X-ray fluorescence core scanner at the University of Massachusetts, Amherst. We subsampled both cores at 1 cm<sup>3</sup> intervals for weight loss-on-ignition analysis<sup>18</sup>. We used XRF and LOI data to align the surface and piston cores on a composite depth scale<sup>18</sup>.

We previously published an age model for this sediment core<sup>18</sup>, and improved upon the age model here through the addition of radiocarbon samples and two cryptotephra. In total, we collected 20 plant macrofossil samples from the surface and piston cores, and the samples were analyzed for radiocarbon at either the Woods Hole NOSAMS facility and the University of California, Irvine Keck AMS facility. We analyzed the geochemistry of five tephra layers in the sediment core using microprobe, which provided further age constraints (see Supplementary Information, Supplementary Fig. 1, Supplementary Table 2, and Supplementary Data File 1). We created an age model using Bacon in R<sup>39</sup> and the IntCal13 calibration curve<sup>40</sup>. 11 radiocarbon age reversals occur, and we removed them from the final age model (Supplementary Table 1). A modern radiocarbon age occurs at 18 cm composite depth, which we assigned an age of 0BP, and we applied a linear age model from 18 cm depth to the core surface, which was assigned an age of -65BP. No sedimentary or geochemical features discussed occur in this extrapolated interval, so this extrapolation does not affect our interpretations. We attribute the change in sedimentation rate in the upper 18 cm to the building of a dam that occurred in 1980.

**Biomarkers.** We collected 68 sub-samples with a thickness of 1 cm from the piston and surface cores, spanning an interval of more concentrated organic matter as evidenced by high LOI values from 29–53 cm. We processed biomarker samples based on established methods<sup>41</sup>. We freeze-dried and homogenized the sediments, and extracted the lipids using a Dionex accelerated solvent extractor. We used a 9:1 dichloromethane (DCM):methanol solution to extract lipids at 100 °C. We saponified the total lipid extract using a KOH solution. We separated the acid and neutral fractions via multiple liquid-liquid extractions using toluene, followed by acidification of the sample and recovery by subsequent liquid-liquid extraction. We separated the neutral fraction into apolar, ketone, and polar fractions via alumina

oxide column chromatography, using elutions of 9:1 DCM:hexane, 1:1 DCM:hexane, and 1:1 DCM:methanol, respectively. We added 20 µL of androstano to each polar fraction, which we derivatized using bis-trimethylsilyl tri-fluoroacetamide (BSTFA) for 4 h at 70 °C. We performed a solvent exchange to toluene in order to avoid precipitation of silica in sample vials.

We analyzed the biomarker samples using an Agilent 7890 A gas chromatograph equipped with a mass selective detector (MSD) and a 30 m-long DB-5 capillary column with an internal diameter of 250 µm. We set the initial GC oven temperature to 90 °C (1.5 min hold), then ramped the temperature to 265 °C at 12 °C/min, then ramped to 288 °C at 0.8 °C/min, and then ramped to 300 °C at 10 °C/min and held for 20 min. We setup the run in single-ion-monitoring (SIM)/scan mode, so that scan data could be used for compound identification, and SIM data could be used for compound quantification. We identified compounds by comparing sample mass spectra to a standard solution containing cholesterol, coprostanol, epicoprostanol, and a-stigmastanol, and other published mass spectra. We quantified compounds by determining the response factor for characteristic ions, as measured in SIM mode, across a range of standard concentrations (see Supplementary Table 4 and Supplementary Fig. 5 for further information regarding SIM method setup and compound identification).

**Sedimentary ancient DNA.** We took 14 sediment samples from the EI-P-01 core across the disturbance interval. We sent 14 total sediment samples in two batches to the UCSC Paleogenomics Center's ancient DNA lab. We homogenized sediment prior to subsampling 500 mg for DNA extraction. We extracted DNA from the 14 samples in two batches, each batch alongside one extraction negative control which did not include any soil following the Rohland extraction protocol<sup>42</sup>.

We amplified plant and mammal DNA from each sediment sample using metabarcoding of trnL and 16S gene regions. We also amplified 3 PCR negatives per primer set. We amplified plant DNA with primers that have been previously tested on ancient samples<sup>43</sup> that target an 85 base pair region of the trnL gene. We amplified mammalian DNA using 16S primers which target a 140 base pair region<sup>44</sup>. We used qPCR to reduce inhibition effects on PCR and optimize the number of cycles used for PCR<sup>45</sup>. We performed qPCR with the Qiagen Multiplex PCR Master Mix to minimize GC bias<sup>46</sup>. We used a qPCR mix as follows: 12.5 µL Qiagen MM, 2 µL of each 2 µM primer, 0.6 µL 1:2000 dilution SYBR Green 1 Dye, 5.9 µL water, and 2 µL extracted DNA. For each of the 14 samples, we created a 1:0, 1:1, and 1:3 dilution series with water. We amplified each of the 14 samples at three dilutions in triplicate and for both primers. We chose the dilution per sample to use in PCR with the lowest cT value, and chose sample-specific cycle numbers per primer by the point at which exponential amplification ended. We amplified our samples with 35–44 cycles with trnL and 40–44 cycles with 16Smamm. With the sample-specific dilution and cycle number, we amplified the 14 samples and 2 extraction replicates in triplicate for both primers following the '2-step' protocol<sup>46</sup>. We performed metabarcoding PCR following the same conditions as the qPCR without SYBR Dye. We performed the second indexing PCR which attached dual index primers using Kappa HiFi polymerase (Roche, Pleasanton, CA, USA) (reaction volumes: 12.5 µL Kapa HiFi, 5.5 µL water, 1 µL of each 10 µM forward and reverse index, and 5 µL purified PCR product). We sequenced libraries on an Illumina NextSeq 2x150bp run. To filter data, cluster sequences based on ASV's and assign ASV's to taxa, we used the Anacapa pipeline<sup>47</sup>. We used the decontam package in R (v1.1.0)<sup>48</sup> to compare taxonomic composition of samples and negative controls and remove any observed contamination. Reads generated from 16S amplifications of negative controls were all human, and reads generated from trnL amplifications were all from plants not present in our samples, except for Poaceae unassigned to lower taxonomic rank reads. We rarefied our trnL data to 5000 reads per sample with the `rarefy_even_depth()` function of phyloseq, and applied a minimum read threshold of five, where a minimum of five reads are required to consider a taxa assigned to a sample a positive ID. While there is no standard minimum read threshold that is standard across the environmental DNA community, a threshold of five is commonly used<sup>49,50</sup>. Rarefaction is similarly not standardized across the environmental DNA field<sup>51</sup>, however, it is necessary to compare the relative composition of samples, and in this case is a more conservative approach.

## Data availability

All data are available in the Supplementary Data File 1, and also via the PANGAEA data archive, titled "Sedimentary ancient DNA, fecal biomarker, and tephrochronology from Eidisvatn, Faroe Islands."

Received: 5 January 2021; Accepted: 5 November 2021;

Published online: 16 December 2021

## References

- Arge, S. V. Viking Faroes : Settlement, Paleoeconomy, and Chronology. *J. N. Atl.* **7**, 1–17 (2014).
- Arge, S. V. et al. Viking and medieval settlement in the Faroes: People, place and environment. *Hum. Ecol.* **33**, 597–620 (2005).
- Tierney, J. J. *Dicuillus: Liber de mensura orbis terrae* (Dublin, 1967).
- Jakobsen, J. *Greinir og Ritgerðir* (Torshavn, 1957).
- Dahl, S. The Norse Settlement of the Faroe islands. *Med. Archaeol.* **14**, 60–73 (1970).
- Als, T. D. et al. Highly discrepant proportions of female and male Scandinavian and British Isles ancestry within the isolated population of the Faroe Islands. *Eur. J. Hum. Genet.* **14**, 497–504 (2006).
- Arge, S. V. The Landnám in the Faroes. *Arct. Anthropol.* **28**, 101–120 (1991).
- Church, M. J. et al. The Vikings were not the first colonizers of the Faroe Islands. *Quat. Sci. Rev.* **77**, 228–232 (2013).
- Johansen, J. Pollen Diagrams from the Shetland and Faroe Islands. *New Phytologist* **75**, 369–387 (1975).
- Johansen, J. Studies in the vegetational history of the Faroe and Shetland Islands. *Annales Societas Scientiarum Færoensis Supplementum* **11** (1985).
- Hannon, G. E. & Bradshaw, R. H. W. Impacts and timing of the first human settlement on vegetation of the Faroe Islands. *Quat. Res.* **54**, 404–413 (2000).
- Hannon, G. E. et al. Human impact and landscape degradation on the Faroe Islands. *Biol. Env.: Proc. Royal Irish Acad.* **101B**, 129–139 (2001).
- Hannon, G. E. & Bradshaw, R. H. W. Human impact and landscape change at Argisbrekka. In *Saeteren ved Argisbrekka*, 306–323 (Froðskapur, Torshavn, 2007).
- Hannon, G. E., Bradshaw, R. H. W., Bradshaw, E. G., Snowball, I. & Wastegård, S. Climate change and human settlement as drivers of late-Holocene vegetational change in the Faroe Islands. *The Holocene* **5**, 639–647 (2005).
- Hannon, G. E., Rundgren, M. & Jessen, C. A. Dynamic early Holocene vegetation development on the Faroe Islands inferred from high-resolution plant macrofossil and pollen data. *Quat. Res.* **73**, 163–172 (2010).
- Lawson, I. T. et al. Human impact on an island ecosystem: pollen data from Sandoy, Faroe Islands. *J. Biogeogr.* **35**, 1130–1152 (2008).
- Hannon, G. E., Bradshaw, R. H. W. & Wastegård, S. Rapid vegetation change during the early Holocene in the Faroe Islands detected in terrestrial and aquatic ecosystems. *J. Quat. Sci.* **18**, 615–619 (2003).
- Curtin, L. et al. Holocene and Last Interglacial climate of the Faroe Islands from sedimentary plant wax hydrogen and carbon isotopes. *Quat. Sci. Rev.* **223**, 105930 (2019).
- Johansen, J. *Plantago lanceolata* in the Faroe Islands and its significance as indicator of prehistoric settlement. *Froðskaparrit; annales Societatis Scientiarum Færoensis* (1989).
- Mahler, D. L. D. Argisbrekka: New Evidence of Shielings in the Faroe Islands. *Acta archaeologica* **61**, 60–72 (1991).
- Bull, I. D., Lockheart, M. J., Elhmmali, M. M., Roberts, D. J. & Evershed, R. P. The origin of faeces by means of biomarker detection. *Env. Int.* **27**, 647–654 (2002).
- D'Anjou, R. M., Bradley, R. S., Balascio, N. L. & Finkelstein, D. B. Climate impacts on human settlement and agricultural activities in northern Norway revealed through sediment biogeochemistry. *Proc. Natl. Acad. Sci. USA* **109**, 20332–7 (2012).
- White, A. J. et al. Fecal stanols show simultaneous flooding and seasonal precipitation change correlate with Cahokia's population decline. *Proc. Natl. Acad. Sci.* **116**, 1–6 (2019).
- Willerslev, E. et al. Diverse Plant and Animal Genetic Records from Holocene and Pleistocene Sediments. *Science* **300**, 791–795 (2003).
- Crump, S. E. et al. Arctic shrub colonization lagged peak postglacial warmth: Molecular evidence in lake sediment from Arctic Canada. *Global Change Biology* **25**, 4244–4256 (2019).
- Parducci, L. et al. Glacial survival of boreal trees in Northern Scandinavia. *Science* **338**, 1083–1087 (2012).
- Anderson-Carpenter, L. L. et al. Ancient DNA from lake sediments: Bridging the gap between paleoecology and genetics. *BMC Evol. Biol.* **11**, 30 (2011).
- Giguët-Coxev, C. et al. Long livestock farming history and human landscape shaping revealed by lake sediment DNA. *Nature communications* **5**, 3211 (2014).
- Schmid, M. M., Dugmore, A. J., Vésteinsson, O. & Newton, A. J. Tephra isochrons and chronologies of colonisation. *Quaternary Geochronol.* **40**, 56–66 (2017).
- de Wet, G. A. Arctic and North Atlantic paleo-environmental reconstructions from lake sediments. PhD Thesis, University of Massachusetts, Amherst (2017).
- Prost, K., Birk, J. J., Lehnendorff, E., Gerlach, R. & Amelung, W. Steroid biomarkers revisited - Improved source identification of faecal remains in archaeological soil material. *PLoS ONE* **12**, 1–30 (2017).
- Malmros, C. Exploitation of Local, Drifted and Imported Wood by the Vikings on the Faroe Islands. *Bot. J. Scotland* **46**, 552–558 (1994).
- Johansen, J. Survey of geology, climate and vegetational history. *A Century of Tree-Planting in the Faroe Islands* (1989).

34. Johansen, J. Cereal cultivation in Mykines, Faroe Islands AD 600. *Danm. Geol. Unders.*, Årøbog, 93–103 (1978).
35. Wastegård, S., Björck, S., Grauert, M. & Hannon, G. E. The Mjávotn tephra and other Holocene tephra horizons from the Faroe Islands: A link between the Icelandic source region, the Nordic Seas, and the European continent. *Holocene* **11**, 101–109 (2001).
36. Bender Jørgensen, L. The introduction of sails to Scandinavia: Raw materials, labour and land. In N-TAG TEN. Proceedings of the 10th Nordic TAG conference at Stiklestad, Norway 2009, **2399**, 173–181 (2012).
37. Westerdahl, C. Sails and the Cognitive Roles of Viking Age Ships (Routledge, 2015).
38. Bill, J. *Viking Age ships and seafaring in the West* (Routledge, 2010).
39. Blaauw, M. & Christen, M. Flexible paleoclimate age-depth models using an autoregressive gamma process. *Bayesian Analysis* **6**, 457–474 (2011).
40. Reimer, P. J. et al. IntCal13 and Marine13 Radiocarbon Age Calibration Curves 0–50,000 Years cal BP. *Radiocarbon* **55**, 1869–1887 (2013).
41. Birk, J. J., Dippold, M., Wiesenberg, G. L. B. & Glaser, B. Combined quantification of faecal sterols, stanols, stanones and bile acids in soils and terrestrial sediments by gas chromatography - mass spectrometry. *J. Chromatography A* **1242**, 1–10 (2012).
42. Rohland, N., Glocke, I., Aximu-Petri, A. & Meyer, M. Extraction of highly degraded DNA from ancient bones and teeth. *Nature Protocols* **13**, 2447–2461 (2018).
43. Taberlet, P. & Coissac, E. Towards next-generation biodiversity assessment using DNA metabarcoding. *Mol. Ecol.* **33**, 2045–2050 (2012).
44. Taylor, P. G. Reproducibility of ancient DNA sequences from extinct Pleistocene fauna. *Mol. Biol. Evol.* **13**, 283–285 (1996).
45. Murray, D. C., Coghlan, M. L. & Bunce, M. From benchtop to desktop: Important considerations when designing amplicon sequencing workflows. *PLoS ONE* **10**, 1–21 (2015).
46. Nichols, R. V. et al. Minimizing polymerase biases in metabarcoding. *Mol. Ecol. Res.* **18**, 927–939 (2017).
47. Curd, E. E. et al. Anacapa Toolkit: An environmental DNA toolkit for processing multilocus metabarcode datasets. *Methods Ecol. Evol.* **10**, 1469–1475 (2019).
48. Davis, N. M., Proctor, D. M., Holmes, S. P., Relman, D. A. & Callahan, B. J. Simple statistical identification and removal of contaminant sequences in marker-gene and metagenomics data. *Microbiome* **6**, 1–14 (2018).
49. West, K. M. et al. eDNA metabarcoding survey reveals fine-scale coral reef community variation across a remote, tropical island ecosystem. *Mol. Ecol.* **29**, 1069–1086 (2020).
50. Bessey, C. et al. Maximizing fish detection with eDNA metabarcoding. *eDNA* **2**, 493–504 (2020).
51. Weiss, S. et al. Normalization and microbial differential abundance strategies depend upon data characteristics. *Microbiome* **5**, 1–18 (2017).

## Acknowledgements

We dedicate this paper to the late Simún Arge from the Faroe Islands National Museum in Tórshavn. Simún provided invaluable advice and support throughout this project, and will be sorely missed. We also thank Tom McGovern and Seth Brewington for their encouragement in the early stages of this research. We also thank Nicole DeRoberts and

Helen Habicht for their assistance with fecal biomarker analysis, Josh Kapp and Shard Milne for their assistance with *sed*aDNA analysis, and D. Andrew Merriwether, Sarah Gilleland and Cassie Koch for assistance with *sed*aDNA extractions. We thank two reviewers whose comments improved the manuscript.

This project was supported by a grant (9740-15) from the National Geographic Society to RSB, by National Science Foundation grants BCS-1623627 to RSB, BCS-23595 to WJD, BCS-1623458 to NLB, and ICER-1850949 to BS, and by HHMI Professor award GT10483 to BS.

## Author contributions

R.S.B., W.J.D., and N.L.B. designed the study. R.S.B., W.J.D., N.L.B., G.A.D., and J.B. collected the sediment cores. L.C., S.S., and G.A.D. performed laboratory analyses under the supervision of W.J.D. and B.S. L.C., R.S.B., W.J.D., N.L.B., and S.S. wrote the manuscript with contributions from all authors.

## Competing interests

The authors declare no competing interests.

## Additional information

**Supplementary information** The online version contains supplementary material available at <https://doi.org/10.1038/s43247-021-00318-0>.

**Correspondence** and requests for materials should be addressed to Lorelei Curtin or William J. D'Andrea.

**Peer review information** Communications Earth & Environment thanks Ana Duggan and the other, anonymous, reviewer(s) for their contribution to the peer review of this work. Primary Handling Editors: Rachael Rhodes, Joe Aslin. Peer reviewer reports are available.

**Reprints and permission information** is available at <http://www.nature.com/reprints>

**Publisher's note** Springer Nature remains neutral with regard to jurisdictional claims in published maps and institutional affiliations.



**Open Access** This article is licensed under a Creative Commons Attribution 4.0 International License, which permits use, sharing, adaptation, distribution and reproduction in any medium or format, as long as you give appropriate credit to the original author(s) and the source, provide a link to the Creative Commons license, and indicate if changes were made. The images or other third party material in this article are included in the article's Creative Commons license, unless indicated otherwise in a credit line to the material. If material is not included in the article's Creative Commons license and your intended use is not permitted by statutory regulation or exceeds the permitted use, you will need to obtain permission directly from the copyright holder. To view a copy of this license, visit <http://creativecommons.org/licenses/by/4.0/>.

© The Author(s) 2021

# Supplemental Information: Sedimentary DNA and molecular evidence for early human occupation of the Faroe Islands

Lorelei Curtin<sup>1\*</sup>, William J. D'Andrea<sup>1\*</sup>, Nicholas L. Balascio<sup>2</sup>,  
Sabrina Shirazi<sup>3</sup>, Beth Shapiro<sup>3</sup>, Gregory A. de Wet<sup>4,†</sup>,  
Raymond S. Bradley<sup>4</sup>, Jostein Bakke<sup>5</sup>

<sup>1</sup>Lamont-Doherty Earth Observatory, Palisades, NY, USA.

<sup>2</sup>Department of Geology, William & Mary, Williamsburg, VA, USA.

<sup>3</sup>Department of Ecology and Evolutionary Biology, University of California,  
Santa Cruz, CA, USA.

<sup>4</sup>Department of Geosciences, University of Massachusetts, Amherst, MA, USA.

<sup>5</sup>Department of Earth Science, University of Bergen, Bergen, Norway.

<sup>†</sup>Present Address: Department of Geosciences, Smith College, Northampton, MA, USA.

\*To whom correspondence should be addressed: [lcurtin@uwyo.edu](mailto:lcurtin@uwyo.edu),  
[dandrea@ldeo.columbia.edu](mailto:dandrea@ldeo.columbia.edu)

## Supplementary Methods

### Tephra analysis

Four visible tephra and two cryptotephra horizons were identified in the Eiðisvatn record. Cryptotephra were isolated by digesting 1 cm<sup>3</sup> samples in 10% H<sub>2</sub>O<sub>2</sub> to remove organics, washing the remaining sediment over a 20 µm sieve, and then subjecting samples to heavy-liquid density separations to isolate material with two density ranges, 2.3-2.5 g/cm<sup>3</sup> and 2.5-2.85 g/cm<sup>3</sup><sup>1,2</sup>. After inspection of tephra under a transmitted light microscope major oxide geochemical compositions were determined using wavelength-dispersive spectroscopy on an ARL-SEMQ electron microprobe equipped with six wavelength-dispersive spectrometers and a Bruker 5030 SDD energy-dispersive spectrometer at the Concord University Microanalytical Laboratory (WV, USA) using a 6 µm beam diameter, 14 kV accelerating voltage, and 10 nA



beam current. Reported data are non-normalized oxide concentrations with each datum representing a single analysis of one tephra shard.

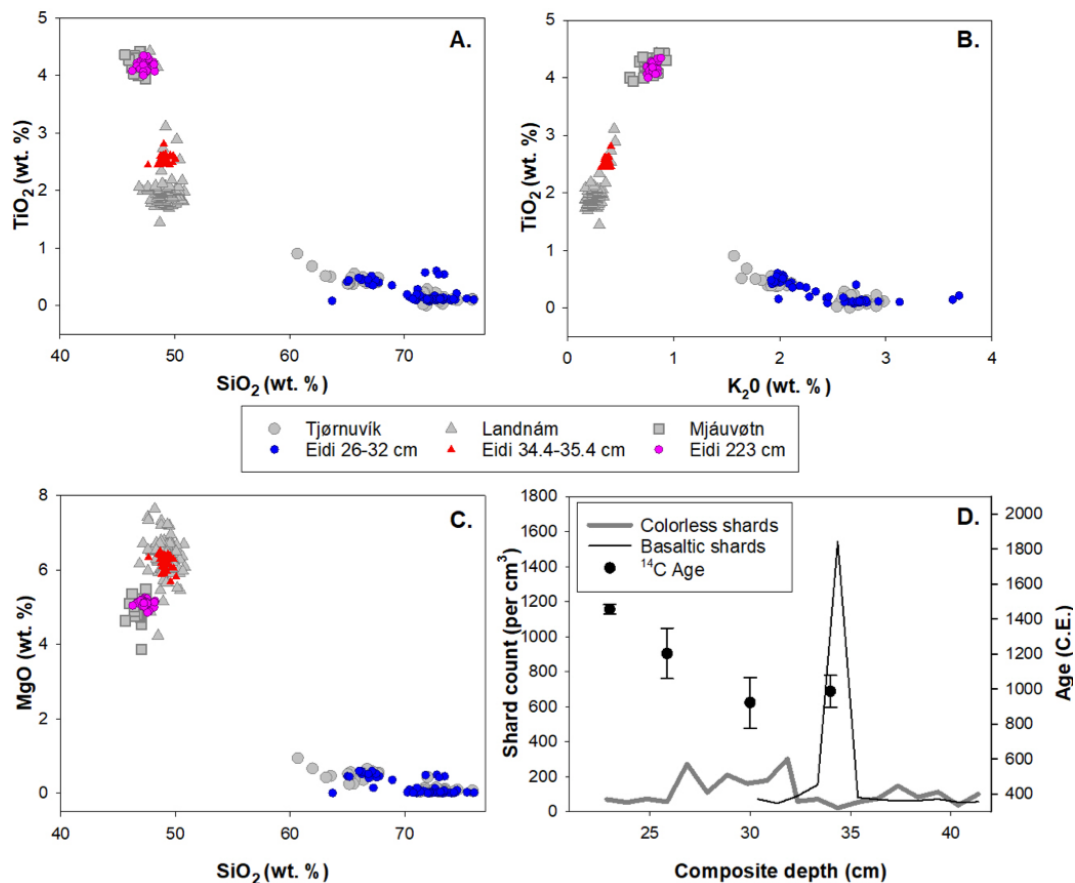
As reported by Curtin et al. (2019)<sup>3</sup>, microprobe analysis indicated that three of these tephra horizons were Hekla-Selsund, Hekla 4, and Saksunarvatn with associated ages of 3,750, 4,260, and 10,200 cal. years B.P., respectively. Here we also identify the Mjáuvøtn Tephra ( $\sim 6,600 \pm 68$  cal year B.P.<sup>4</sup>), and two cryptotephra that are likely associated with the Tjørnuvík and Landnám Tephra ( $\sim 1150$ s cal yr B.P. [800s CE]) and  $\sim 1073$  cal yr B.P. [877 CE], respectively) (as reviewed by Wastegård et al., 2018<sup>5</sup>) (Supplementary Table 2).

The basaltic Mjáuvøtn Tephra was found as a dark  $\sim 1$  mm-thick layer at 223 cm and the geochemistry resembles tephra found at other sites in the Faroe Islands attributed to this eruption of the Icelandic Katla volcanic system<sup>4,6</sup> (Supplementary Figure 1). A sharp peak in dark green to brown shards up to 1600 shards/cm<sup>3</sup> was found from 34.4-35.4 cm in the heavier density range, and a lower and more diffuse peak in colorless, vesicular shards was found from 26-32 cm in the lighter density range (Supplementary Figure 1). The geochemistry of shards from 34.4-35.4 cm is similar to the basaltic phase of the Landnám Tephra, although TiO values of all of the shards analyzed (n=35) are at the upper end of the typical range for this tephra (Supplementary Table 2, Supplementary Figure 1). Tephra with intermediate to rhyolitic composition were found from 26-32 cm (830-1050 cal yr B.P.; CE 1120-900). The geochemical composition of these tephras are similar to glass shards derived from the Hekla volcano and possibly represent the presence of the Tjørnuvík Tephra. The Tjørnuvík Tephra has been identified as a distinct cryptotephra horizon at Tjørnuvík on Streymoy<sup>7</sup>, in a bog at Eiði on Eysturoy<sup>6</sup>, and in a peat core from Suduroy<sup>8</sup>. At two of these sites it has been found with tephra shards from the basaltic phase of the Landnám Tephra and tentatively ascribed to a Hekla eruption in the 9th century. This is roughly consistent with the modeled age of this interval in our record. However, it has also been suggested that the Tjørnuvík Tephra may not be a primary deposit but rather reworked

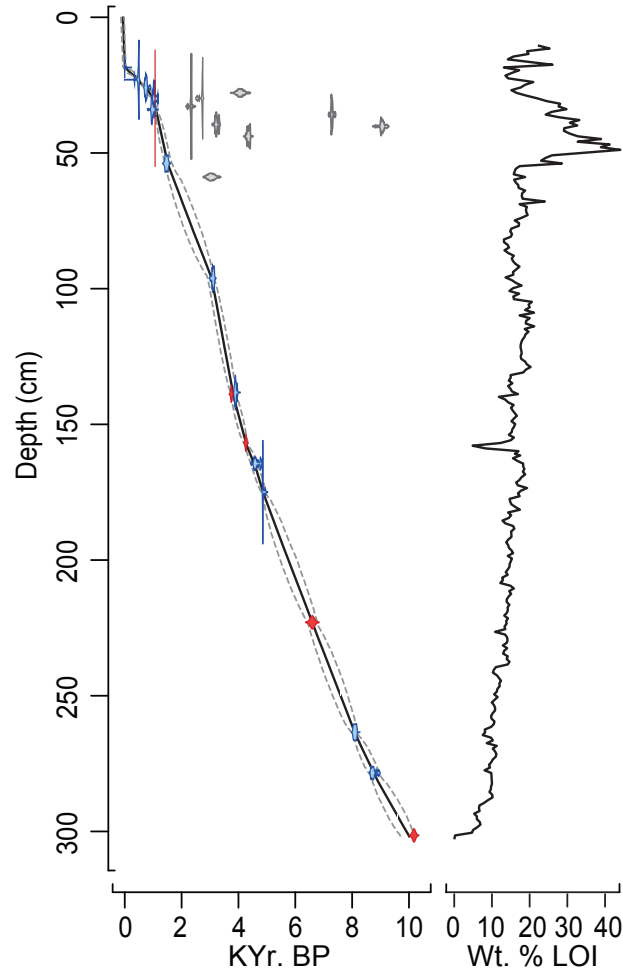
from earlier, more significant, deposits of Hekla 4 and Hekla S eruptions mobilized due to soil erosion during initial human settlement of the Faroe Islands<sup>5</sup>. This may be the case at our site considering the range of anomalously old radiocarbon ages across this interval.

In the Eiðisvatn age model we use the Hekla-Selsund, Hekla 4, Mjáuvøtn and Saksunarvatn Tephra as age-control points. However, because of our tentative correlation to the Landnám Tephra geochemistry and the suggestions by others that the Tjørnuvík Tephra may not be a primary deposit, we did not use them as age-control points. Nevertheless, both cryptotephrae are consistent with the age model that we have adopted.

## Supplementary Figures

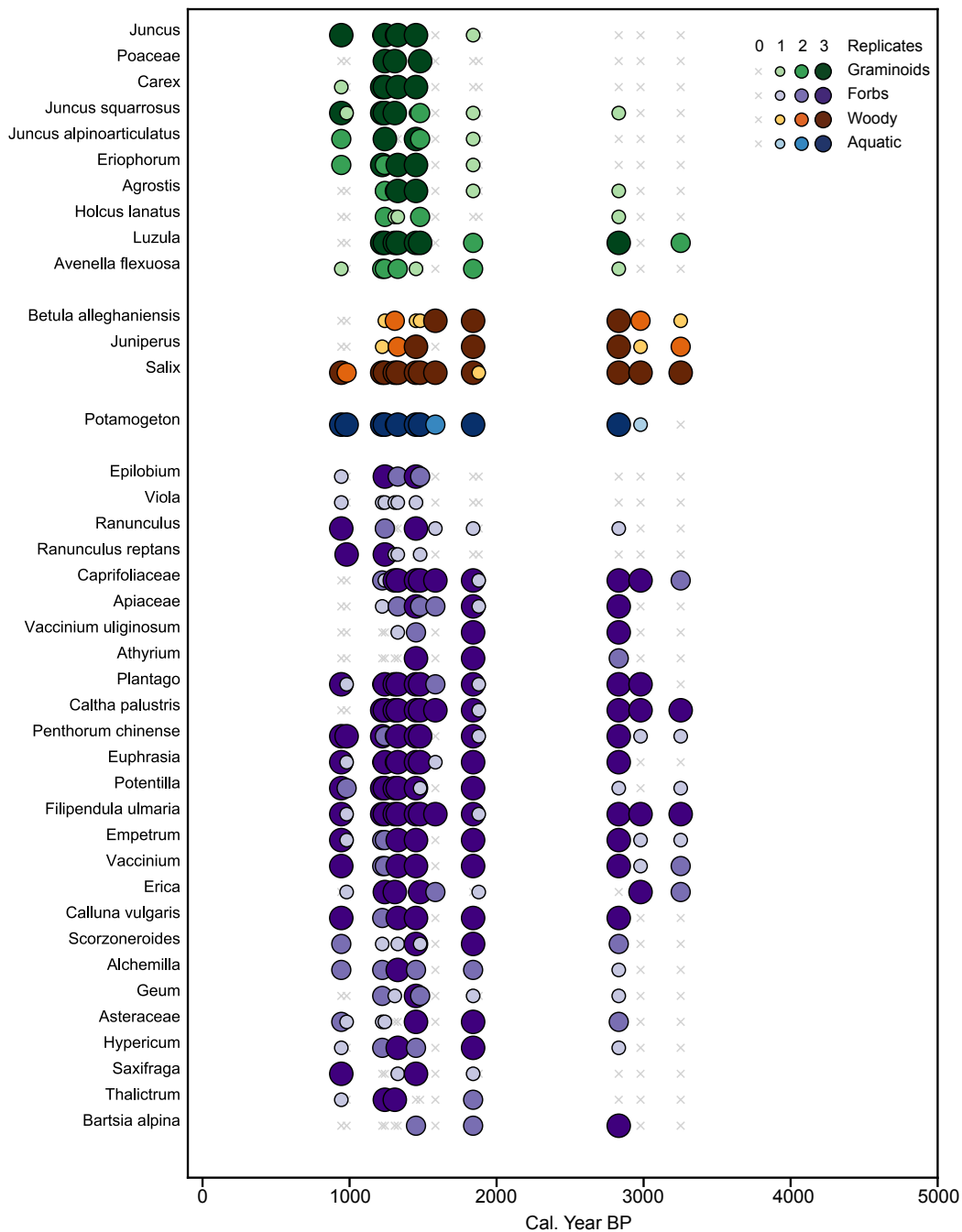


**Supplementary Figure 1: Tephra geochemical data.** Geochemical data from tephra samples analyzed from the Eiðisvatn sediment compared to data from tephra attributed to the Tjörnurvík<sup>7-9</sup>, Landnám<sup>7-11</sup>, and Mjáuvøtn<sup>9</sup> Tephra. Shard counts and radiocarbon ages (error bars are 95% confidence intervals for radiocarbon-based ages) also shown across the interval searched for cryptotephra (D.).

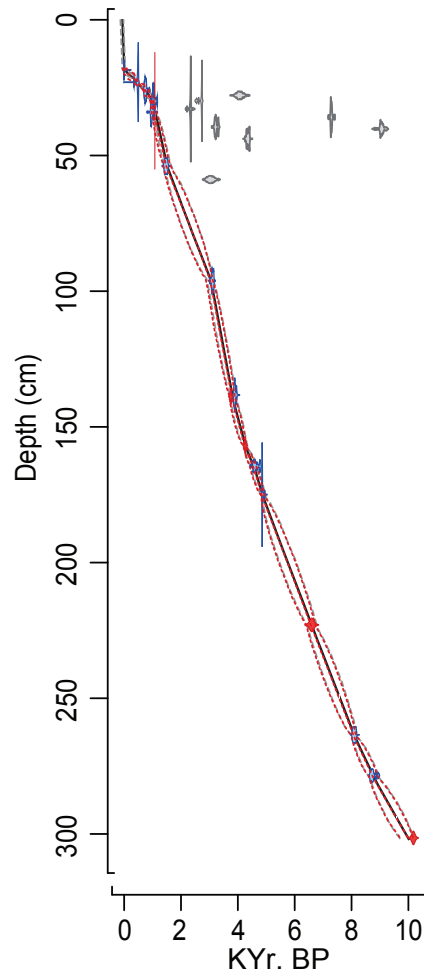


**Supplementary Figure 2: Eiðisvatn age model and downcore weight % loss-on-ignition.** Blue data points are probability distribution functions for radiocarbon ages used in the age model, calibrated using the IntCal13 calibration curve<sup>12</sup>. Red data points are probability distribution functions for tephrochronological ages. Grey data points are probability distribution functions for radiocarbon ages that were excluded from the final age model. Solid black line in age model is the weighted median age as determined by Bacon in R<sup>13</sup>. Dashed line indicates 95% confidence interval for the age model.



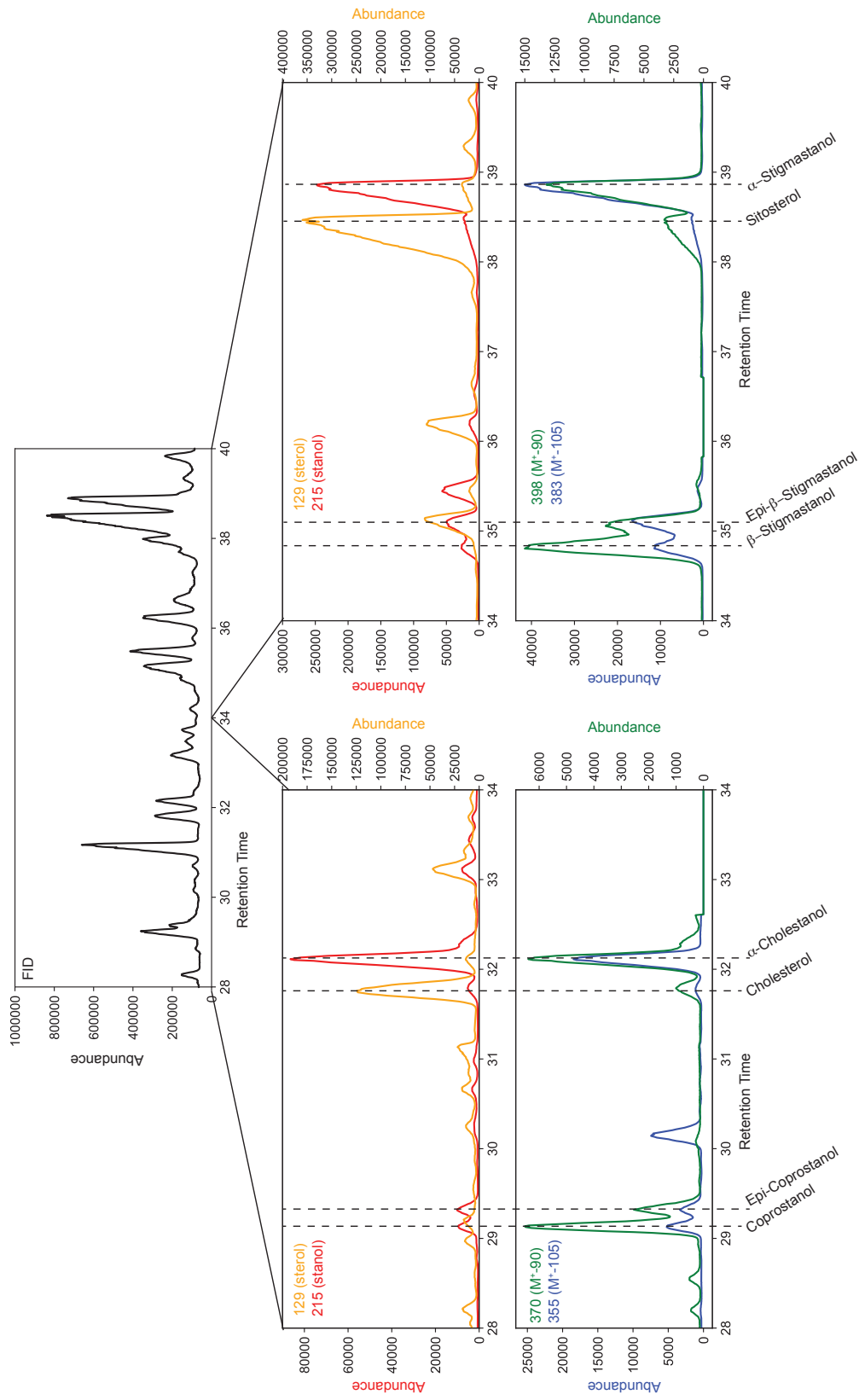


**Supplementary Figure 3: Frequency of plant DNA identification for all genera identified.** Frequency of plant DNA identification for all genera identified. Plant DNA data points are scaled by size and color relative to the number of PCR replicates in which the specific plant genus was positively identified (threshold of 5 reads or greater). X indicates samples where that genera was not identified.



**Supplementary Figure 4: Eiðisvatn age model, with and without the Landnám tephra.**

Age model with the Landnám tephra appears as in Supplementary Figure 1, with black line indicating weighted mean age model and grey dashed lines indicating 95% confidence intervals. Age model with the Landnám tephra removed is in red dashed lines. The age models are indistinguishable, and the maximum age difference is 29.1 years.



**Supplementary Figure 5: FID and characteristic ion chromatograms for fecal sterol molecules in an Eidsvatn sediment sample.** Fecal biomarkers were quantified using a combined SIM/Scan method on a GC-MSD/FID system. Uppermost panel shows FID trace. Left panels show SIM ion traces for  $m/z$  = 129, 215, 355, and 370. Right panels show SIM ion traces for  $m/z$  = 129, 215, 398, and 383. Note that each ion was plotted on its own y-axis scale to facilitate identification.

## Supplementary Tables

**Supplementary Table 1:** Chronological data for age model

Core	Material	Depth (cm)	<sup>14</sup> C Age	Error	Median Calibrated Age
	Sediment Surface	0	-65		-65
EI-D-01-15	Terrestrial Macrofossil	18.5	0		-3
EI-D-01-15	Terrestrial Macrofossil	23	410	15	493
EI-P-01-15	Terrestrial Macrofossil	25.86	840	30	747
EI-P-01-15	Terrestrial Macrofossil	27.86	3720	70	4070*
EI-P-01-15	Terrestrial Macrofossil	29.86	2575	20	2737*
EI-D-01-15	Terrestrial Macrofossil	30	1145	15	1027
EI-P-01-15	Terrestrial Macrofossil	32.86	2320	20	2343*
EI-P-01-15	Landnám Tephra	33	-	1	1073
EI-D-01-15	Terrestrial Macrofossil	34	1055	35	962
EI-P-01-15	Terrestrial Macrofossil	35.86	6355	20	7284*
EI-D-01-15	Terrestrial Macrofossil	39.5	3030	20	3227*
EI-D-01-15	Terrestrial Macrofossil	40.2	8110	45	9055*
EI-P-01-15	Terrestrial Macrofossil	43.86	3915	20	4358*
EI-P-01-15	Terrestrial Macrofossil	53.86	1580	35	1469
EI-P-01-15	Terrestrial Macrofossil	58.86	2900	80	3043*
EI-P-01-15	Terrestrial Macrofossil	96.16	2945	15	3109
EI-P-01-15	Terrestrial Macrofossil	138.26	3595	15	3895
EI-P-01-15	Hekla-S Tephra	138.86	-	20	3750
EI-P-01-15	Hekla-4 Tephra	156.86	-	20	4260
EI-P-01-15	Terrestrial Macrofossil	164.46	4100	30	4611
EI-P-01-15	Terrestrial Macrofossil	174.96	4310	15	4857
EI-P-01-15	Mjáuvötn Tephra	222.96	-	68	6600
EI-P-01-15	Terrestrial Macrofossil	263.46	7290	30	8102
EI-P-01-15	Terrestrial Macrofossil	278.46	7925	20	8731
EI-P-01-15	Saksunarvatn Tephra	301.46	-	49	10176

\* indicates anomalously old radiocarbon ages that were excluded from the final age model



**Supplementary Table 2:** Geochemical composition of glass shards isolated from the Eiðisvatn record compared to tephra identified at other Faroe Islands sites.

Sample		SiO <sub>2</sub>	TiO <sub>2</sub>	Al <sub>2</sub> O <sub>3</sub>	FeO	MnO	MgO	CaO	Na <sub>2</sub> O	K <sub>2</sub> O	P <sub>2</sub> O <sub>5</sub>	Cl	BaO	Total
<b>Eiði 26-32 cm</b>	<i>Mean</i>	70.96	0.23	13.41	3.06	0.11	0.17	1.99	4.68	2.51	0.05	0.07	0.08	97.30
(n=54)	<i>1 σ</i>	3.04	0.17	0.98	1.53	0.04	0.22	0.87	0.43	0.41	0.05	0.04	0.03	2.41
<b>Tjørnuvík</b>	<i>Mean</i>	69.80	0.27	13.64	3.93	0.14	0.26	2.32	4.01	2.41	-	-	-	96.77
(n=39) <sup>1</sup>	<i>1 σ</i>	4.19	0.21	0.85	2.44	0.07	0.24	1.11	0.33	0.46	-	-	-	1.34
<b>Eiði 33 cm</b>	<i>Mean</i>	49.09	2.55	13.47	12.38	0.21	6.20	10.70	2.58	0.37	0.27	0.02	0.01	97.84
(n=35)	<i>1 σ</i>	0.45	0.08	0.15	0.16	0.01	0.20	0.36	0.11	0.02	0.01	0.01	0.01	0.61
<b>Landnám</b>	<i>Mean</i>	49.11	2.02	13.36	1.47	0.21	6.37	10.97	2.59	0.27	-	-	-	97.37
(n=15) <sup>2</sup>	<i>1 σ</i>	0.83	0.43	0.37	0.62	0.04	0.53	0.66	0.24	0.11	-	-	-	1.05
<b>Eiði 223 cm</b>	<i>Mean</i>	47.33	4.17	12.95	14.30	0.23	5.10	9.59	2.99	0.80	0.50	0.04	0.02	98.02
(n=28)	<i>1 σ</i>	0.42	0.09	0.15	0.36	0.01	0.09	0.32	0.13	0.03	0.03	0.00	0.01	0.77
<b>Mjáuvøtn</b>	<i>Mean</i>	46.70	4.19	12.88	14.46	0.28	4.90	10.05	3.07	0.77	-	-	-	97.31
(n=19) <sup>3</sup>	<i>1 σ</i>	0.46	0.15	0.45	0.41	0.10	0.35	0.53	0.30	0.53	-	-	-	0.91

<sup>1</sup> Tjørnuvík A geochemical data from Tephabase<sup>7-9</sup>

<sup>2</sup> Basaltic phase of the Landnám tephra from Tephabase<sup>8-11</sup>

<sup>3</sup> Mjáuvøtn tephra geochemical data from Wastegård et al., 2001<sup>9</sup>.

**Supplementary Table 3:** Ages (cal. yr. BP) of settlement horizons with two age models

	Depth	Age Model Includes Landnam Tephra			Age Model Without Landnam Tephra		
		Weighted Mean Age	Min Age	Max Age	Weighted Mean Age	Min Age	Max Age
Wt. % LOI Increase	53.86	1515	1415	1670	1507	1408	1669
Biomarker Increase	50	1433	1317	1565	1420	1293	1551
Sheep DNA	50.88	1451	1344	1580	1440	1325	1571

**Supplementary Table 4:** SIM method setup

<b>Group</b>	<b>Start/ End time</b>	<b>Compound</b>	<b>RT</b>	<b>M<sup>+</sup></b>	<b>M<sup>+</sup> - 90</b>	<b>M<sup>+</sup> - 105</b>	<b>Other ions</b>	<b>SIM ions for group</b>
<b>1</b>	Start: 24.5 End: 30.0	Coprostanol	29.1	460	370	355	215	460, 370, 355, 215, 129
		Epicoprostanol	29.3	460	370	355	215	
<b>2</b>	Start: 30.0 End: 32.6	Cholesterol	31.7	458	368	353	129	384, 370, 369, 368, 355, 353, 215, 129
		$\beta$ -Campestanol	32.0	474	384	369	215	
		Epi- $\beta$ -Campestanol	32.2	474	384	369	215	
		$\alpha$ -cholestanol	32.0	460	370	355	215	
<b>3</b>	Start: 32.6 End: 33.8	Brassicasterol	33.0	470	380	365	129	470, 380, 365, 215, 129
<b>4</b>	Start: 33.8 End: 36.0	$\beta$ -Stigmastanol	34.7	488	398	383	215	398, 384, 383, 382, 369, 367, 215, 129
		Epi- $\beta$ -Stigmastanol	34.9	488	398	383	215	
		Campesterol	35.0	472	382	367	129	
		$\alpha$ -campestanol	35.3	474	384	369	215	
<b>5</b>	Start: 35.7 End: 36.7	$\beta$ -Stigmasterol	36.0	484	394	379	129	484, 394, 379, 215, 129
<b>6</b>	Start: 36.7 End: 39.0	$\beta$ -Sitosterol	38.0	486	396	381	129	398, 396, 383, 381, 129, 215
		$\alpha$ -Stigmastanol	38.5	488	398	383	215	

## Supplementary References

1. Turney, C. S. M., Harkness, D. D. & Lowe, J. J. The use of microtephra horizons to correlate Late-glacial lake sediment successions in Scotland. *Journal of Quaternary Science* **12**, 525–533. ISSN: 0267-8179 (1997).
2. Blockley, S. P. E. *et al.* A new and less destructive laboratory procedure for the physical separation of distal glass tephra shards from sediments. *Quaternary Science Reviews* **24**, 1952–1960. ISSN: 0277-3791 (Sept. 2005).
3. Curtin, L. *et al.* Holocene and Last Interglacial climate of the Faroe Islands from sedimentary plant wax hydrogen and carbon isotopes. *Quaternary Science Reviews* **223**, 105930. ISSN: 0277-3791 (2019).
4. Olsen, J. & Gudmundsdóttir, E. R. Revised age estimate of the Máuvøtn tephra A on the Faroe Islands based on Bayesian modelling of  $^{13}\text{C}$  dates from two lake sequences. *Journal of Quaternary Science* **25**, 612–616 (2010).
5. Wastegård, S. *et al.* Towards a Holocene tephrochronology for the Faroe Islands, North Atlantic. *Quaternary Science Reviews* **195**, 195–214 (2018).
6. Wastegård, S., Björck, S., Grauert, M. & Hannon, G. E. The Mjáuvøtn tephra and other Holocene tephra horizons from the Faroe Islands: a link between the Icelandic source region, the Nordic Seas, and the European continent. *The Holocene* **11**, 101–109. ISSN: 09596836 (2001).
7. Hannon, G. E., Hermanns-Auðardóttir, M. & Wastegård, S. Human Impact at Tjørnuvík in the Faroe Islands. *Fróðskaparrit* **46**, 215–228 (1998).
8. Wastegård, S. Early to middle Holocene silicic tephra horizons from the Katla volcanic system, Iceland: new results from the Faroe Islands. *Journal of Quaternary Science* **17**, 723–730 (2002).
9. Wastegård, S., Björck, S., Grauert, M. & Hannon, G. E. The Mjáuvøtn tephra and other Holocene tephra horizons from the Faroe Islands: A link between the Icelandic source region, the Nordic Seas, and the European continent. *Holocene* **11**, 101–109. ISSN: 09596836 (2001).
10. Boyle, J. Towards a Holocene tephrochronology for Sweden: Geochemistry and correlation with the North Atlantic tephra stratigraphy. *Journal of Quaternary Science* **19**, 103–109. ISSN: 02678179 (2004).
11. Larsen, G., Dugmore, A. & Newton, A. Geochemistry of historical-age silicic tephras in Iceland. *Holocene* **9**, 463–471. ISSN: 09596836 (1999).
12. Reimer, P. J. *et al.* IntCal13 and Marine13 Radiocarbon Age Calibration Curves 0–50,000 Years cal BP. *Radiocarbon* **55**, 1869–1887. ISSN: 00382222 (2013).
13. Blaauw, M. & Christen, M. Flexible paleoclimate age-depth models using an autoregressive gamma process. *Bayesian Analysis* **6**, 457–474 (2011).